Effect of Adhesion Layer on Morphology and Optical Properties of Self-Organized Metal Nanostructures

Victor Ovchinnikov
MICRONOVA Nanofab
School of Electrical Engineering, Aalto University
Espoo, Finland
e-mail: Victor.Ovchinnikov@aalto.fi

Abstractð **The inexpensive fabrication method of self-organized metal nanostructures with adhesion layer over large area is proposed. The method combines dry etching using a self-organized mask to prepare a template and directional metal deposition on the elevated part of the obtained template. The technique peculiarities were studied during fabrication of metal lace-like nanostructures prepared with Ti layer and without it. The results demonstrate the overall difference in transmittance and reflectance spectra of the samples due to presence of Ti layer. Surface enhanced Raman spectroscopy (SERS) experiments were performed with methylene blue and confirmed decreasing of SERS intensity of the gold nanostructures with adhesion layer. The obtained results can be used in fabrication of self-organized metal nanostructures with controllable adhesion.**

Keywords-self-organized; fabrication method; metal nanostructure; random array; plasmonics; SERS substrate

I. INTRODUCTION

Metal nanostructures have greatly broadening applications in many areas of chemical and biological sensing [1], subwavelength imaging[2], metamaterials[3] and etc. The best studied and attractive from the theoretical point of view are periodic arrays of metal nanoparticles, but their mass production is a challenging task, which waits for the decision. Traditional semiconductor technology provides reliable and reproducible process flows, but its acceptance as a general fabrication tool of metal nanostructures has been hindered by two obstacles: (1) limited resolution of optical lithography and (2) lack of dry etching processes for most metals. That is why, the dominant fabrication method of regular metal nanostructures is electron beam lithography (EBL) together with lift-off removing of useless metal. However, by this process is highly difficult to obtain features smaller than 50 nm. Additionally, the extensive processing time needed in EBL for fabrication of arrays of nanostructures over large areas makes it expensive and time-consuming.

As alternative to serial EBL, several non-lithography or self-organizing methods exist to produce nanostructures in parallel way. These techniques create structures with a random nature, i.e. arrays of metal nanostructures with randomly distributed size and space of elements. Active areas beyond 1×1 cm^2 and low price are inherent to the techniques, but functional properties of nanostructures deteriorate, narrowing application area of random arrays. In spite of this, the random nanostructures are used as a catalyst in carbon nanotube growth [4], as a light trapping layer in thin film solar cells [5], as magnetic nanodot arrays [6], as surface enhanced Raman scattering (SERS) substrates [7] and sensors [8]. As examples of non-lithography techniques can be mentioned nanosphere lithography [9], using of porous alumina template [10], oblique angle deposition [11] and etc. They have own application areas, but the most attractive method is generation of metal nanostructures by self-assembling on the surface with poor adhesion, e.g., Au-Ag nanoislands on glass [12]. The method possesses nanometer range resolution, cheapness and compatibility with semiconductor technology.

Unfortunately, broad application of this self-organizing technique is restrained by poor adhesion of produced metal structures to a dielectric substrate and limited set of structure configurations (mainly round-shaped islands and holes). By the nature of phenomenon, self-organization occurs in a thin layer of noble metal on dielectric substrate at non-equilibrium thermodynamic conditions without firm contact between metal and substrate. The fabricated random arrays can be easily damaged during rinsing in de-ionized water and are not suitable for incorporation in more complicated devices. It is therefore desirable to improve the adhesion properties of self-organized structures, e.g., by introducing of intermediate adhesion layer.

Lift-off based methods, including EBL, inherently include an adhesion layer to preserve functional metal elements during mask removing. Therefore, nanostructures without adhesion layer cannot be produced by these methods and direct estimation of influence of intermediate layer on the functional properties is impossible. As a consequence, there are only experimental results for different (non-zero) thicknesses of adhesion layer in nanostructures or comparison of flat (non-patterned) metal films with and without adhesion layer [13, 14].

In this paper, a fabrication method of self-organized metal nanostructures with adhesion layer over large area is considered. The method was used to create lace-like Au and Ag nanostructures with and without Ti layer on glass and silicon substrates. This gave an opportunity to study the influence of adhesion layer on morphology and optical properties of fabricated nanostructures by direct comparison.

 ISBN: 978-1-61208-151-9

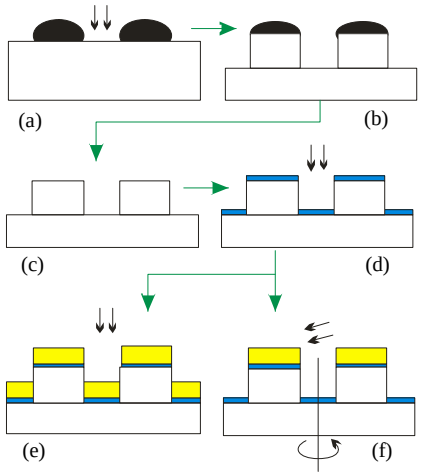

Figure 1. Fabrication process of metal nanostructures with intermediate layer.

Despite of vast transformation of optical response due to presence of Ti layer, it was demonstrated that gold lace-like nanostructures with gap width below 10 nm can be used as effective SERS substrates.

In the subsequent sections, the description of the fabrication method is presented, followed by detailed sample preparation and measurement procedures. After presenting of SEM images of the obtained nanostructures, the reflectance and SERS spectra are discussed.

II. FABRICATION METHOD

The idea of the method consists in fabrication of a nanostructure template from a substrate and directional deposition of metal layers on the template. For template preparation any patterning method, providing vertical sidewalls can be used: lithography and etching, self-organizing structures and etching, direct writing by laser or focused ion beam [15, 16]. In this work, self-organized gold nanostructures are used as a mask for anisotropic dry etching of the substrate (Fig. 1a,b). To create the mask a thin gold layer is evaporated on the substrate at low deposition rate. The film has lace-like structure, if the gold thickness does not exceed 15 nm and the adhesion between metal and the substrate is poor. Other metals or additional annealing after deposition can be used to modify the mask morphology. For example, silver provides round-shaped nanoislands with size and separation controlled by annealing [17]. The poor adhesion of gold to a substrate limits the etching methods for patterning of the nanostructures, e.g., wet etching must be eliminated. On the other hand, dry etching still can be used, because surface tension forces and interlayer diffusion of liquid have no place. Additionally, dry etching, e.g., reactive ion etching (RIE), provides vertical (Fig. 1b) sidewalls of the nanostructures.

In the next step the residues of the mask metal are removed by selective wet etching to obtain a nanotemplate made of the substrate material (Fig. 1c). The template elements replicate the shape and size of the mask (e.g., lace-lice structure) and, in general, can have any lateral geometry (e.g., disks for silver self-organizing mask). The template is then covered by a thin adhesion layer of easily oxidized metal (e.g., Ti or Cr). At atmospheric ambient the adhesion layer, which is not protected by upper metal is readily oxidized and does not affect on functional properties of nanostructures. It is important to deposit the adhesion layer only on horizontal surfaces of the template and leave the sidewalls uncovered (Fig. 1d) to avoid firm contact of the second metal with vertical surfaces. This requirement is fulfilled by using a physical vapour deposition (e.g., evaporation) at normal incidence. Due to poor adhesion of the metal to sidewalls, it can be easily removed by rinsing in ultrasound bath.

The final step is coating of the template with a functional metal layer, for example gold or silver. It is done immediately after deposition of the adhesion layer to prevent possible oxidation of the latter. This time metal coating of the template can be made in two ways. In the first one, the metal is evaporated in a direction normal to the wafer surface, which simultaneously deposits metal on the elevated nanostructure planes and the backplane (Fig. 1e). In the second way, the metal is deposited at the angle (Fig. 1f) on the rotating or unmovable template. The rotation provides uniform covering of structure tops, while static deposition leads to 3D nanostructures, in which sidewalls and tops are covered simultaneously. The deposition angle Ŭis chosen to be large enough to minimize metal coating of backplane. In this case, the height h of the sidewall metallization (measured from structure top) can be roughly estimated as [18]

$$h_m = \frac{l}{\tan\alpha}, \qquad (1)$$

where l is the average space between structures. In practice, deviations from (1) are happened, especially for small l, when sidewalls are not become covered by metal at all.

III. EXPERIMENTAL

The samples were fabricated on precleaned squares of borosilicate glass and oxidized Si (100) with size 22×22×0.5 mm^3. The cleaning procedure begins with sonicating in acetone and 2-propanol. After that the samples were RCA-1 cleaned for 10 minutes and processed in oxygen plasma during 1 minute. The pretreatment is needed to equalize the surface conditions through the whole substrate. The Si pieces with a 60 nm thick layer of SiO_2 were used to optimize the whole process, because it makes possible to observe the fabricated nanostructures with SEM. At the same time all process steps lead to identical results on glass and on oxide.

The metal films were deposited in e-beam evaporation system IM-9912 (Instrumentti Mattila Oy) with adjustable substrate inclination and rotation speed at base pressure of 4×10^{-7} Torr and at room temperature of the substrate. The deposition rates for each film were measured using quartz crystal microbalance. The RIE of template was done in a 13.56 MHz driven parallel electrode reactor Plasmalab 80

 ISBN: 978-1-61208-151-9

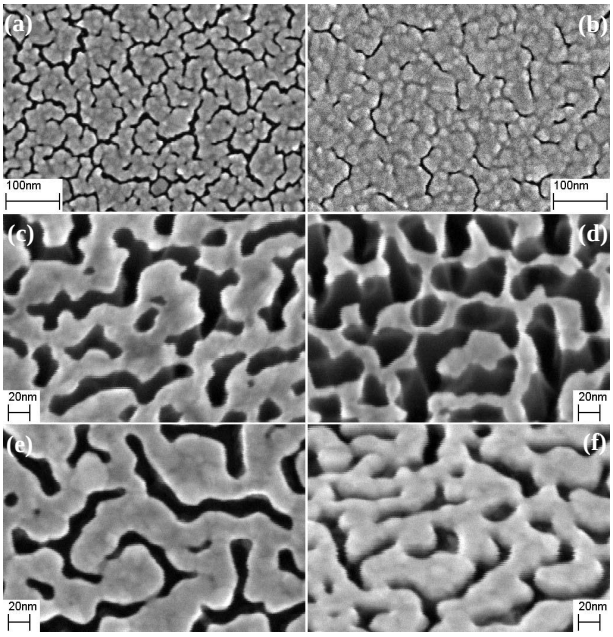

Figure 2. SEM images of lace-like nanstructures after main process steps: (a,b) 10 and 15 nm thick gold films; (c,d) RIE for 20 and 25 minutes, respecticely; plain (e) and tilted (f) views of 16 nm thick gold nanostructures.

Plus (Oxford Instruments Plasma Technology). An anisotropic etching process based on fluorine chemistry (gas mixture CF_4:CHF_3=1:3) was used for glass and SiO_2 etching. The etching experiments were performed at a total gas flow of 80 sccm, pressure 30 mTorr and rf power 40 W. The remaining gold was removed in aqua regia (1:3 volume mixture of 69% HNO3 and 37% HCl, respectively) during 20 s at room temperature, leaving a lace-like structures from SiO_2 or glass.

Plane-view and tilted at 30° SEM images of the samples were observed with Zeiss Supra 40 field emission scanning electron microscope. Transmittance and reflectance measurements at normal incidence were carried out using PerkinElmer Lambda 950 UV-VIS spectrometer in the spectral range from 300 to 850 nm. All reflectance spectra were collected with integrating sphere as a detector. Raman scattering was studied in WITec Alpha 300 Raman microscope equipped with a Nd:YAG (532 nm) laser as an excitation source. Methylene blue (MB) at the concentration of 3×10^{-4} M was used as a test molecule with water as a solvent. MB solution was dropped on SERS samples using a pipette and then dried in air to obtain a uniform molecule deposition.

IV. RESULTS

To check the method lace-like nanostructures from gold and silver with Ti adhesion layer were fabricated. Both metals have poor adhesion to glass, but are very attractive for plasmonic applications. Fig. 2 illustrates most important steps in the nanofabrication. As a self-organized mask was used a 10 nm thick gold layer deposited at 0.5 Å/s. In

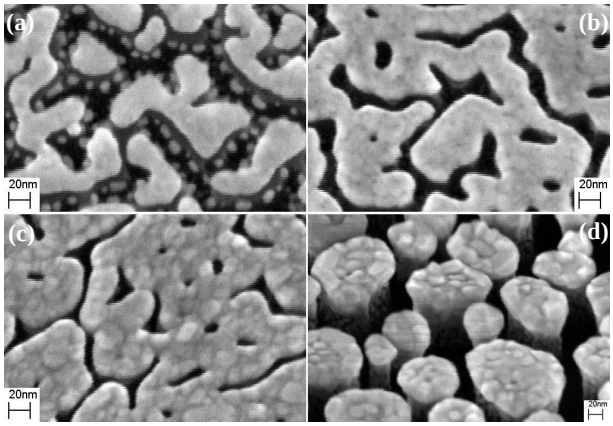

Figure 3. SEM images of nanostructures: (a,b) 8 nm thick gold nanostructures without Ti and with Ti, respectively; (c,d) 8 nm thick silver and 16nm gold nanostructures with Ti deposited at 70° with rotation.

contrast to well known self-organizing masks from Au and Ag [19], annealing is not required; the film is used as-deposited to preserve feature sizes as small as possible. Such a procedure results in lace-like structure, consisting of channels (depressions) and protrusions (projections) (Fig.2a). Average width of the first ones is about 7 nm, the second ones ï 30 nm. Protrusion and channel sizes can be tuned by gold thickness, substrate temperature and deposition rate. As an example, in Fig. 2b is shown the 15 nm thick gold film deposited at the same conditions, which has smaller width and density of the channels. Unfortunately, mask thickness is only a little larger than the thickness of the deposited metal and limits the depth of RIE (Fig. 2c,d). Till the certain moment during etching the mask pattern is unchanged (Fig. 2c) and channel widths in SiO_2 and gold are equal. Further etching increases channel width and destroys flatness of protrusion tops (Fig. 2d), what is connected with gold mask erosion during ion bombardment. Additionally, it leads to deviation of sidewall profile from vertical. The maximum etching depth of 75 nm reached after 25 minutes of RIE (Fig. 2d), resulted in increasing of channel width to 25 nm. Deposition of 1 nm thick Ti and 16 nm thick gold layers on the structure shown in Fig. 2d was done in static mode (Fig.1e,f) and led to shrinking of the channel width back to 7 nm.

To further clarify the mechanism of nanostructure metallization, the gold film was also deposited on the template without Ti adhesion layer (Fig. 3a). Metal nanostructures do not exactly follow the template pattern, like in case of Ti layer (Fig. 3b); instead of this, they are broken in shorter segments and surrounded by small nanoclusters. It looks that on the tops of protrusions there are favorable thermodynamic conditions for gold migration to the centre of isolated areas. This facilitates formation of large islands in the middle of protrusions due to non-wetting property of Au on SiO_2 surface. At the same time, protrusion edge is a favorable place for cluster nucleation, but due to limited amount of gold, these clusters are small in size. In

 ISBN: 978-1-61208-151-9

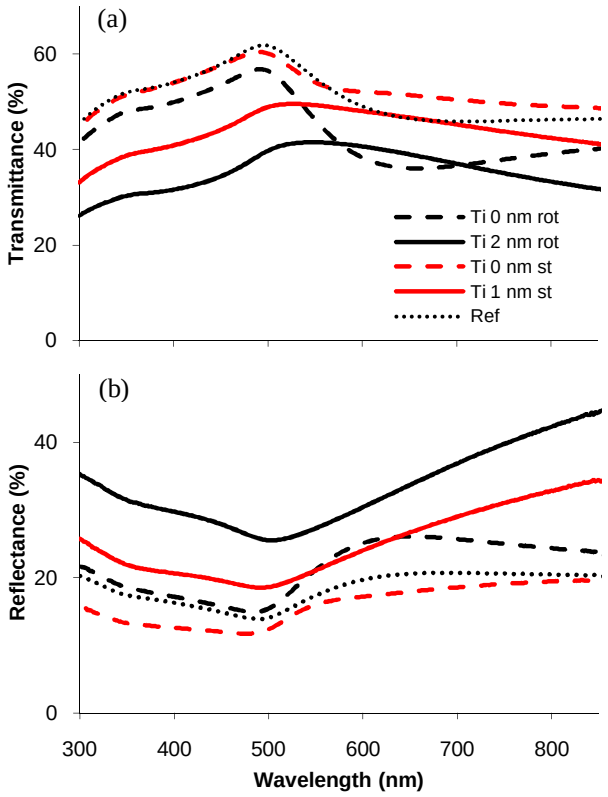

Figure 4. Transmittance (a) and reflectance (b) spectra of 8 nm thick gold nanstructures with Ti and without Ti on glass deposited at normal angle (st) or at 70° with rotation (rot). Ref ï 8 nm gold on glass without Ti.

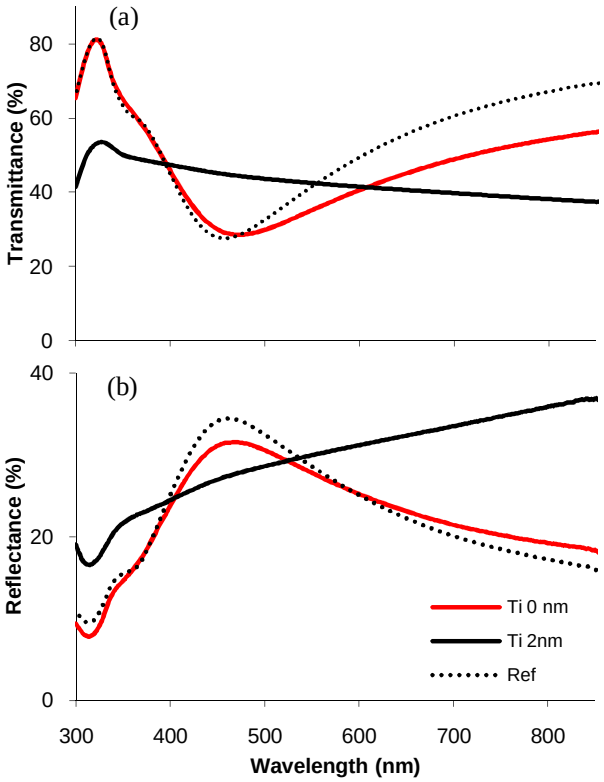

Figure 5. Transmittance (a) and reflectance (b) spectra of 8 nm thick silver nanstructures with Ti and without Ti on glass deposited at 70° with rotation. Ref ï 8 nm silver on glass without Ti.

case of Ti/Au layer (Fig. 3b), surface diffusion of gold atoms is limited and the film grows uniformly above protrusion tops. Growth rate of the metal film is higher on the protrusion edge, what leads to formation of rim around nanostructure (Fig. 2f). The rim shadows sidewalls from metal deposition, decreases channel width and diminishes amount of metal on the backplane. The lateral growth rate of the rim can be controlled by tilting and rotating the substrate during deposition. Fig. 3c, d display lace-like Ag structures similar ones shown Fig. 3b and SiO_2 pillars covered by gold, respectively. In both cases deposition was done on rotating substrate at the angle 70^0. As a result of rotation, the channel width is smaller in comparison with static deposition (Fig. 3b) and diameter of metal disks on the pillar tops is 40 nm larger than pillar diameter.

Whatever the deposition result, samples appear extremely attractive for plasmonic and especially SERS applications. This supposition is confirmed by transmittance and reflectance of gold nanostructures on glass substrate shown in Fig. 4. To make the template, glass was etched during 16 minutes, what was resulted in channel depth about 65 nm. The reference sample is 8 nm thick gold film deposited on plain surface of glass substrate. Optical properties for wavelength shorter 500 nm reflect interband transitions of *d*-electrons in gold and are not connected with surface plasmon resonance (SPR). All samples consist of strongly interacting structures with size deviation, what leads to broadening and shifting of resonance peaks inherent to gold nanoparticles [20].

Samples without Ti layer demonstrate SPR near 650 nm, which is stronger for sample deposited at angle and weaker for sample deposited at normal direction. But spectra of structures with Ti layer are totally different. Low transmittance in the blue half of spectra is caused by high reflectance and justifies narrowing of the channels (increasing metal covered area). Redshift and broadening of maximum transmittance band near 500 nm is attributed to influence of Ti layer absorbance, which monotonically decreases for visible range of wavelength. Modification of red half of spectra is connected with flattening of metal nanostructures (Fig. 3) and increased interaction between oscillators due to shrinking of channels. The result is strong and non-uniform splitting of SPR, observed as featureless spectrum.

Transmittance and reflectance of silver nanostructures, prepared on the same template as gold ones are shown in Fig. 5. As well as in case of gold nanostructures, reference sample and lace-like nanostructures without Ti demonstrate similar spectra. There are longitudinal SPR at 460 nm and transverse SPR at 360 nm. However, after introducing of Ti layer only weak sings on these SPRs can be visible on practically flat spectra due to nanostructure shape variation and dampening caused by Ti layer. It cost to note, that for wavelength longer than 600 nm the appearance of Ti/Au and

 ISBN: 978-1-61208-151-9

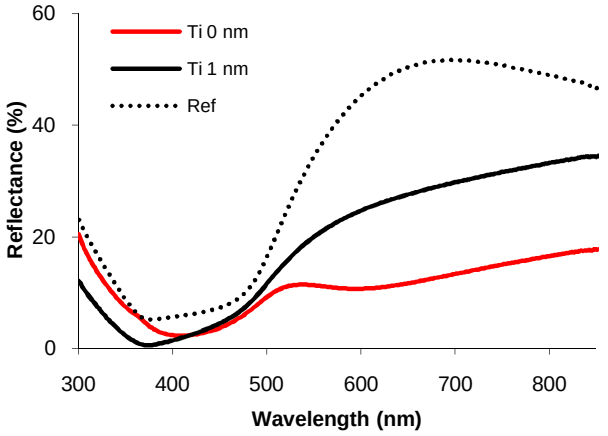

Figure 6. Reflectance spectra of 8 nm thick gold nanstructures with and without Ti on Si/SiO_2 deposited at normal angle. Ref ï 11 nm gold on the same substrate.

Ti/Ag spectra is practically the same (Fig. 4, 5), in contrast to the behavior of Au and Ag reference samples. It can be considered as evidence of template (not metal) effect on optical properties of nanostructures.

Reflectance of gold nanostructures, prepared in the same process as glass samples, but on silicon substrate, is shown in Fig.6. Spectra demonstrate interference picture in the system Si/SiO_2 modified by absorption in nanostructure layer. Due to this, SPRs manifest themselves as minimums of reflectance and can be visible in pure Au sample (600 nm) and extrapolated in reference sample (beyond of 900 nm). SPRs are redshited in comparison with glass samples (Fig. 4b), due to high effective dielectric constant of environment, modified by Si substrate. At the same time redshift in pure Au sample (no Ti layer) is much less than in reference sample, because the etched channels partly compensate effect of Si substrate on permittivity of environment. Low reflectance in the left part of spectra (shorter 500 nm) is attributed to absorption in gold together with destructive

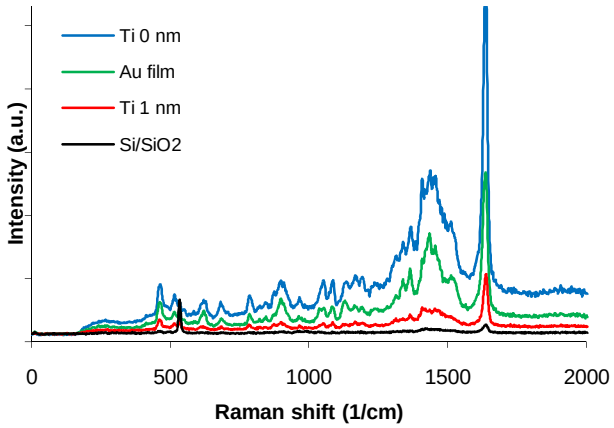

Figure 7. SERS spectra of methylene blue for the gold nanostructures desribed in Fig. 6.

interference in SiO_2 layer. The special point at 375 nm is connected with peak of reflectance in crystalline Si. As in case of glass substrate, sample with adhesion layer is featureless.

The raw Raman spectra of MB on Si/SiO_2 samples, represented by reflectance spectra in Fig. 6 are shown in Fig. 7 (blue and red lines). The peak at 530 cm^{-1} corresponds to the Raman scattering of the crystalline Si substrate. Black and green spectra present the Raman scattering of the bare Si/SiO_2 and 11 nm thick gold layer on Si/SiO_2. It is not surprise, that the maximum enhancement effect on Raman scattering demonstrates sample without Ti layer. Indeed, this sample possesses SPR (600 nm) close to SERS excitation wavelength (532 nm). Relatively strong SERS activity is also attributed to plain substrate with Au film. But SERS intensity of the sample fabricated with Ti layer exceeds only the intensity of bare oxide layer. This difference clearly indicates that plasmonic properties drastically deteriorate by adhesion layer. However, intensity of observed SERS signal for the Ti/Au nanostructures is still enough to distinguish the characteristic peaks of MB at around 1638 and 466 cm^{-1} [21]. This fact and high mechanical stability of the Ti/Au nanostructures make them attractive for embedding in complex devices.

V. CONCLUSIONS

In summary, it has been proposed and demonstrated a new nanofabrication method of self-organized nanostructures both with adhesion layer and without it. With the help of proposed method it has been experimentally studied the influence of Ti adhesion layer on morphology and optical properties of lace-like nanostructures from gold and silver by direct comparison of the samples. The pure gold and silver nanostructures repeat template shape only roughly, concentrating in the middle part of the protrusion tops. The presence of a very thin adhesion layer (e.g., 1 nm thick Ti) leads to uniform covering of top planes of the template and drastically changes nanostructure morphology. As a consequence, SPR features in absorbance and reflectance spectra of the samples with Ti layer are transformed and weakened. Despite of this Ti/Au lace-like nanostructures demonstrate relatively high SERS activity measured with MB as the reference analyte. The obtained results suggest that developed nanofabrication method is promising in preparation of noble metal nanosturctures with adhesive layer to withstand further process treatments. The method is also valuable in fabrication of self-organized nanostructures from any evaporatable metal, e.g., Fe or Al. For future work, it is expected to optimize the template structure and gold thickness for obtaining of maximum SERS enhancement.

REFERENCES

[1] J. N. Anker et al., ñBiosensing with plasmonic nanosensorsò, Nature Materials, vol. 7, 2008, pp. 442 ï 453.

[2] X. Zhang and Z. Liu, ñSuperlenses to overcome the diffraction limitò, Nature Materials, vol. 7, 2008, pp. 435 ï 441.

[3] E. Cortes, L. Mochán, B. S. Mendoza, G. P. Ortiz, ñOptical properties of nanostructured metamaterialsò, Phys. Status Solidi B, vol. 247, 2010, pp. 2102 ï 2107.

[4] Y. F. Guan, A. V. Melechko, A. J. Pedraza, M. L. Simpson and P. D. Rack, ñNon-lithographic organization of nickel catalyst for carbon nanofiber synthesis on laser-induced periodic surface structures,ò Nanotechnology, vol. 18, 2007, pp. 335306 ï 335312.

[5] X. Sheng et al., ñDesign and Non-Lithographic Fabrication of Light Trapping Structures for Thin Film Silicon Solar Cellsò, Adv. Mater. vol. 23, 2011, pp. 843 ï 847.

[6] R M. Tofizur, N. N. Shams, C.-H. Lai, ñNonlithographic fabrication of 25 nm magnetic nanodot arrays with perpendicular anisotropy over a large areaò, J of App. Phys. vol. 105, 2009, pp. 07C112 ï 07C112-3.

[7] M. Fan, G. F.S. Andrade and A. G. Brolo, ñA Review on the fabrication of substrates for surface enhanced Raman spectroscopy and their applications in analytical chemistryò, Analytica Chimica Acta, (in press).

[8] E. Galopin et al., ñShort- and Long-Range Sensing Using Plasmonic Nanostructures: Experimental and Theoretical Studiesò, J. Phys. Chem. C, vol. 113, 2009, pp. 15921 ï 15927.

[9] X. Zhang, L. Zhang, M. Gao, W. Zhou, S. Xie, ñHigh-Resolution Nanosphere Lithography (NSL) to Fabricate Highly-Ordered ZnO Nanorod Arraysò, J. Nanosci. Nanotechnol., , J. Nanosci. Nanotechnol., vol. 10, 2010, pp. 7432 ï 7435.

[10] Y. Piao, H. Kim, ñFabrication of nanostructured materials using porous alumina template and their applications for sensing and electrocatalysisò, J. Nanosci. Nanotechnol., vol. 9, 2009, pp. 2215 ï 2233.

[11] S. Jayawardhana, G. Kostovski, A. P. Mazzolini, and P. R. Stoddart, ñOptical fiber sensor based on oblique angle depositionò, Appl. Opt., Vol. 50, 2011, pp. 155 ï 162.

[12] J. Sancho-Parramon et al., ñOptical and structural properties of Au-Ag islands films for plasmonic applicationsò, Appl. Phys. A, vol. 103, 6 January 2011, Online First, doi: 10.1007/s00339-010-6231-x.

[13] B. Lahiri, R. Dylewicz, R. M. De La Rue, and N. P. Johnson, ñImpact of titanium adhesion layers on the response of arrays of metallic split-ring resonators (SRRs)ò, Optics Express, vol. 18, pp. 11202 ï 11208.

[14] K.W. Vogt, P.A. Kohl, W.B. Carter, R.A. Bell and L.A. Bottomley, ñCharacterization of thin titanium oxide ashesion layers on gold: resistivity, morphology, and compositionò, Surf. Sci., 1993, vol. 301, 1994, pp. 203 ï 213.

[15] K.C. Vishnubhatla et al., ñFemtosecond laser direct writing of gratings and waveguides in high quantum efýciency erbium-doped Baccarat glassò, J. Phys. D, vol. 42, 2009, p. 205106 ï 201112.

[16] R.M. Langford, ñFocused ion beam nanofabrication: a comparison with conventional processing techniquesò, J. Nanosci. Nanotechnol., vol. 6, 2006, pp. 661 ï 668.

[17] C. Eminian, F.-J. Haug, O. Cubero, X. Niquille, C. Ballif, ñPhotocurrent enhancement in thin film amorphous silicon solar cells with silver nanoparticlesò, Progress in Photovoltaics: Research and Applications, vol. 19, 2011, pp. 260 ï 265.

[18] V. Ovchinnikov and A. Shevchenko, ñLarge-Area Arrays of Pillar-Based Metal Nanostructuresò, Proc. Third International Conference on Quantum, Nano and Micro Technologies (ICQNM 2009), The IEEE Computer Society, Feb. 2009, pp. 125-129, doi bookmark: http://doi.ieeecomputersociety.org/10.1109/ICQNM.2009.31.

[19] G. Gupta et al., ñCross-sectional Transmission Electron Microscopy and Optical Characterization of Gold Nanoislandsò, Jpn. J. Appl. Phys., vol. 48, 2009, pp. 080207 ï 080208.

[20] J. Fu and Y. Zhao, ñAu nanoparticle based localized surface plasmon resonance substrates fabricated by dynamic shadowing growthò, Nanotechnology, vol. 21, 2010, pp. 175303 ï 175311.

[21] R. R. Naujok, R. V. Duevel, R. M. Corn, ñFluorescence and Fourier Transform surface-enhanced Raman scattering measurements of methylene blue adsorbed onto a sulfur-modified gold electrodeò, Langmuir, vol. 9, 1993, pp. 1771 ï 1774.

 ISBN: 978-1-61208-151-9